Asian Journal of Civil Engineering (2019) 20:409–419
https://doi.org/10.1007/s42107-018-00114-w

ORIGINAL PAPER

# Study of seismic response characteristics of building frame models using shake table test and considering soil–structure interaction

**Madan Kumar**[1] · **S. S. Mishra**[1]

Received: 4 September 2018 / Accepted: 31 December 2018 / Published online: 19 January 2019


## Abstract

External forces such as earthquake, wind, and blast lead to the deformation of the ground as well as of the supported structures. Ignorance of the influence of soil–structure interaction (SSI) could lead to unsafe design of structures founded particularly on soft soils. To understand the performance of a multi-storey building with varying heights, foundation types, and pile depths under the influence of SSI, a shake table test with earthquake excitation was considered necessary. In this paper, results of a series of shake table test performed on scaled multi-storey building frame models subjected to El-Centro earthquake are presented. The testing was carried out on three building frame models of four, six, and eight storeys. Acceleration, displacement, natural frequency, and damping ratio of the frame models as influenced by the following attributes have been investigated: (1) varying building heights; (2) SSI and fixed base; (3) different types of foundation systems viz. isolated, mat, and pile foundations; and (4) varying pile depths. The experimental investigations considering the SSI effects show that the natural frequency and damping ratio depend on the foundation system of the frame models. It is also observed that the natural frequency and damping ratio decrease with the increase in height of frame model. The investigations show that the pile foundation offers least lateral displacement of the frame models as compared to the isolated and the mat foundations. Empirical formulas are extracted from the test results to estimate the damping.

**Keywords** Shake table test · Soil–structure interaction · Multi-storeyed frame model · Foundation types · Time period · Damping ratio

## Introduction

During earthquakes, responses of the structures such as buildings, bridges, and other ground structures are tremendously affected by the vibrations of the underlying soil layers. Vibrations induced in tall structures are mainly due to ground motions caused by seismic excitations. In this condition, the mechanism that influences the shaking characteristics of the tall structures is the dynamic soil–structure interaction (SSI). The procedure in which the reaction of the soil influences the movement of the structure and movement of the structure influences the reaction of the soil is termed as SSI. Many high-rise buildings in India are supported on pile foundations in soft soil in seismically active areas. The SSI is divided into two parts: inertial interaction and kinematic interaction (Wolf 1985). During an earthquake, the ground motion is transmitted from the soil to the building. The building mass develops an inertia force to resist this change in motion. The inertial force is followed by the modal vibration of the structure throughout the period of the ground shaking. When the shaking stops, the building vibrates freely under the influence of damping and returns to rest ultimately. Due to this, the study of the time period and damping characteristics of the structures is important for design consideration. The SSI is largely influenced by the soil properties. Some researchers have found that SSI lengthens the period (Mishra 2017) and increases the damping of the structural system. Experiences from the past earthquakes show that negligence of the SSI effect will lead to severe damage in buildings and loss of lives especially when the supporting soil is soft. Several numerical as well as experimental studies have been conducted to explore the effects of SSI on structural behavior. Tabatabaiefar and Massumi (2010)

✉ Madan Kumar
madan.ce15@nitp.ac.in

S. S. Mishra
ssmishra@nitp.ac.in

[1] Department of Civil Engineering, National Institute of Technology, Patna, India

carried out numerical study on four types of buildings and three types of soil considering SSI effects and concluded that consideration of SSI effect is important for higher buildings. Tabatabaiefar et al. (2014) investigated further about the effect of SSI on building models through numerical and experimental studies by conducting a series of shaking table test. They observed that the lateral deflection of the model with flexible base had amplified in comparison to the model with fixed base. Chu and Truman (2004) in their study investigated the effect of soil–pile–structure interaction (SPSI) using 3D finite element model by considering infinite element boundary to simulate the radiation damping. Saha et al. (2015) investigated analytically the seismic response of soil–pile–raft–structure system and concluded that the SSI leads to considerable lengthening of the period. Further, from the findings of several researchers (Mishra 2017; Tabatabaiefar and Massumi 2010; Tabatabaiefar et al. 2014; Chu and Truman 2004; Saha et al. 2015; Chau et al. 2009; Badry and Satyam 2016) it has been proved that the SSI is largely influenced by the soil properties. The damages in the building structures have been largely attributed to the local soil properties as reported during Mexico City (Tabatabaiefar and Massumi 2010; Tabatabaiefar et al. 2014; Chu and Truman 2004; Saha et al. 2015; Chau et al. 2009) and Christchurch earthquakes (2011) (Tabatabaiefar et al. 2014; Badry and Satyam 2016). An encouraging work on the estimation of damping and frequency over 80 numbers of existing buildings have been carried out by Gallipoli et al. (2009) using four different methods: horizontal-to-vertical spectral ratio (HVSR), standard spectral ratio (SSR), non-parametric damping analysis (NonPaDAn), and half bandwidth methods (HBW). They reported that these methods estimate damping and frequency with different degrees of accuracy. However, NonPaDAn method gives more reliable results for estimating damping over other methods.

Chau et al. (2009) conducted a shake table test by applying both sinusoidal waves of various magnitudes and also El-Centro earthquake to a soil–pile–structure system. They found that pounding phenomenon occurred between soil and pile due to the development of a gap separation between soil and pile. They observed that the acceleration response of the pile cap increased three times larger than the response of the structure. Hosseinzadeh et al. (2012) conducted shake table tests on 5, 10, 15, and 20 storey models and concluded that the SSI effects decrease by increasing the embedment depth of the foundation in soil. Chen et al. (2017) conducted shake table test on a five-storey reinforced concrete building by subjecting it to earthquake excitations to estimate the predominant period and corresponding equivalent viscous damping ratio. Tang et al. (2014) conducted shake table test on pile foundations in liquefiable sand and overlying soft clay. They investigated the effects of pile pinning, pile diameter, pile stiffness, ground inclination angle, superstructure mass, and pile head restraints on the ground improvement. They observed that a larger pile diameter and fixed pile head restraints contribute to reduce the lateral pile deformation. Kampitsis et al. (2015) carried out 3D pushover analysis on vertical single piles embedded in dry sand. Durante et al. (2013) experimentally validated their analytical results by applying $1g$ acceleration excitation in their shake table test. They observed that the period elongations of the single degree of freedom structure caused by pile–soil interactions may be significant. Ge et al. (2016) studied the dynamic interaction between soil and high-rise buildings by conducting shaking table tests. They observed that the acceleration responses of a group of high-rise buildings are less pronounced than the response of a single isolated building. They also showed that for the El-Centro earthquake, the acceleration response is more obvious for long-period buildings as compared to short-period buildings. Sáez et al. (2013) investigated for the effect of the inelastic dynamic soil–structure interaction (DSSI) of moment-resisting frame buildings.

From the above, it is clear that understanding the effect of pile depth on response of structures to an earthquake is an issue of utmost important. The knowledge of the effects of SSI on massive structures, such as silos, offshore caissons, bridge piers, slender tall structures such as chimneys and towers, and structures supported on very soft soils, is important for designing. In this paper, the study focuses on the determination of natural frequency, damping ratio, acceleration, and displacement responses by shake table testing of building frame models subjected to real earthquake excitation such as El-Centro. The experiment was carried out by considering three steel building frame models of four-, six-, and eight-storey heights. Further, the dynamic characteristics of these models with different foundations (i.e., fixed base, isolated, mat, and pile) are determined and compared mutually. Additionally, all the three building frame models were supported on piles of different depths to understand the effect on response due to different depths of the pile foundation.

The dynamic equations of the motion (Chopra 1995) for a multi-degree of freedom structure subjected to earthquake excitations can be written as:

$$[M]\{\ddot{u}\} + [C]\{\dot{u}\} + [K]\{u\} = -[M]\{\ddot{u}_g\}, \tag{1}$$

where $[M]$, $[C]$, and $[K]$ are the mass, damping, and stiffness matrices of the structure, respectively.$\{\ddot{u}\}$, $\{\dot{u}\}$, and $\{u\}$ are the vectors of relative nodal accelerations, velocities, and displacements of the structure with respect to ground, respectively. $\{\ddot{u}_g\}$ is the vector of ground acceleration.

The factors that influence damage due to shaking of the frame are the shape and size of the structure, the material properties of the structure, the properties of the surrounding soil, and the severity of the ground shaking. Shake table

test on multi-storey frame is highly recommended where the dynamic properties of the prototype structure, such as the natural frequency of the first and higher modes, and the number of storey are simulated.

## Description of the test model

Due to the limitation of the size of the shake table in laboratory, similitude laws have been considered in designing the prototype model. The method establishing the similarity relationship between the model and the prototype is called dimensional analysis method. Similitude formulas and similitude factors of all physical quantities are deduced from Buckingham π theorem. The size of the SSI models was scaled from full-scale buildings and foundations. During modeling, the distortion due to dead and live loads was ignored.

For the study, three types of conventional moment-resisting steel frame building models were used as prototype superstructure of four, six, and eight storeys. The frame building models were assumed to be a residential building with its plan dimension of 3 m × 3 m. The heights of four-, six-, and eight-storey frame models were 1.2, 1.8, and 2.4 m, respectively, corresponding to 12, 18, and 24 m heights of actual building. The plan and elevation of the test models are shown in Fig. 1. For the prototype frame models mild steel plates were used for floor slab and Indian standard angle section (IS 1989) ISA 25 × 25 × 3 was used for the beams and columns of the frame model. The beam ends were filet welded to the column members, insuring rigid joints. The mild steel plates were also connected along their edges with the beam members using intermittent filet welds. The scales considered for the dimensions of the buildings and for piles are $\lambda = 1/10$ and $\lambda = 1/30$, respectively. The model similitudes of physical parameters are defined in terms of the geometric scaling factor $\lambda$, and are summarized in Table 1.

The sizes of isolated, mat, and pile foundations were considered judiciously. The size of the isolated footing of the actual building was 2 m × 2 m and that of the mat footing was 6 m × 6 m. In this study, two cases of different pile depths were adopted. The building considered had 9 m pile depth (abbreviated as Pile#1) in case one, 11.75 m pile depth (abbreviated as Pile#2) in case two. The isolated footings of the steel frame model were of steel plates of dimensions 200 mm × 200 mm × 8 mm. The steel plate dimensions corresponding to mat footing were 340 mm × 340 mm × 8 mm. The piles were of 25-mm-diameter reinforced concrete containing six numbers of 2-mm-diameter steel rods (bicycle spokes). The lengths of Pile#1 and Pile#2 were 300 mm and 375 mm, respectively. The plans and elevations of foundation system considered in the study are shown in Fig. 2.

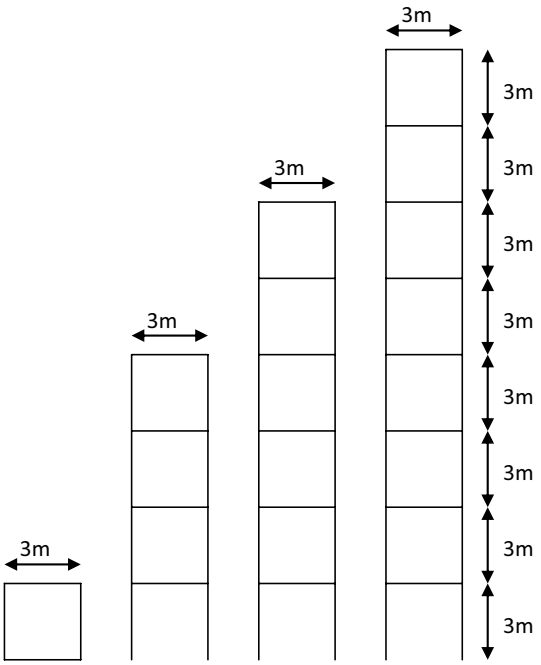


**Fig. 1** Plan and elevation of building frame models

**Table 1** Prototype model scaling factors

| Physical quantity | Dimension | Scaling factors |
|---|---|---|
| Length | L | λ |
| Mass density | $ML^{-3}$ | 1 |
| Acceleration | $LT^{-2}$ | 1 |
| Time | T | $\lambda^{1/2}$ |
| Force | $ML\,T^{-2}$ | $\lambda^3$ |
| Stiffness | $ML^{-1}\,T^{-2}$ | $\lambda^2$ |
| Frequency | $T^{-1}$ | $\lambda^{-1/2}$ |
| Stress | $ML^{-1}\,T^{-2}$ | λ |
| Strain | – | 1 |

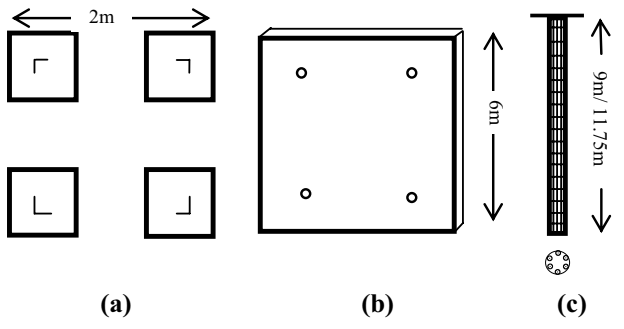


**Fig. 2** Foundation system considered (**a**) isolated footing, (**b**) mat footing, and (**c**) pile

## Properties of soil, simulation of soil boundary condition, and setup for the SSI model and instrumentation

The soil is a critical part to deal with the modeling procedure. The soil collected was a typical soft soil on the basis of *N* value less than 10. The *N* value is a measure of shear strength of soil. It is determined by measuring the penetration resistance of soil to a sampler in terms of the number of blows of a 65 kg hammer falling freely through 75 cm. The number of blows required for second and third 15 cm penetration is termed as *N* value. Soil parameters were derived from laboratory tests to get a broad view of the geotechnical properties. The specific gravity, dry density, and plasticity index of soil obtained from the tests were 2.69, 16.8 kN/m$^3$ and 15%, respectively. This soil is classified as silty-sand soil as per the Indian Standard soil classification (IS 1498).

While considering SSI, the simulation of soil boundary condition plays a key role. The soil theoretically has no boundary (Lu et al. 2002). In shake table test, the soil cannot be placed in an infinite dimension box. Due to variation of system vibration and wave reflection on the boundary, error is bound to occur in the test results. However, due to limitation in container size, laminar soil container (Lu et al. 2002; Turan et al. 2009; Hokmabadi et al. 2015) was designed to simulate the boundary. The dimensions of the flexible soil container properly stiffened were 650 mm × 650 mm × 650 mm. It consisted of steel plates of thickness 3 mm. To minimize the boundary effects, the inner faces of soil container were laminated with a foam layer of thickness 20 mm. To avoid over-deformation during lifting, the container was stiffened with small steel braces. To avoid slippage of the container its base was fixed with the shake table platform using steel fasteners and bolts.

The shake table of the Heavy Structure Lab of the National Institute of Technology Patna has six degrees of freedom capable of giving three translational and three rotational motions along the three orthogonal directions. The shake table platform size is 1.5 m × 1.5 m which is capable of carrying a maximum payload of 1 ton. The shake table can be efficiently run up to 50 Hz, it has the maximum 200 mm displacement limit in horizontal directions. The experimental setups of the four-, six-, and eight-storey frame models are shown in Fig. 3.

To simulate the fixed base condition, the column bases of the frame models were fixed on the shake table platform with bolts. The dynamic response of the building frames was recorded using biaxial accelerometers at each floor level starting from the top floor to pickup the responses of the upper floors. The range of accelerometers used for the experiment was $\pm 5g$. The data were acquired through a data acquisition system consisting of 24 channels with an acquisition rate of 200 data per second. The recorded output accelerations were used to obtain the displacements of the structure with the help of Seismosignal software (2011). The Seismosignal software computes velocity and displacement through integration of acceleration data using the trapezoidal rule. Filtering and baseline corrections were also applied in obtaining the displacement curves.

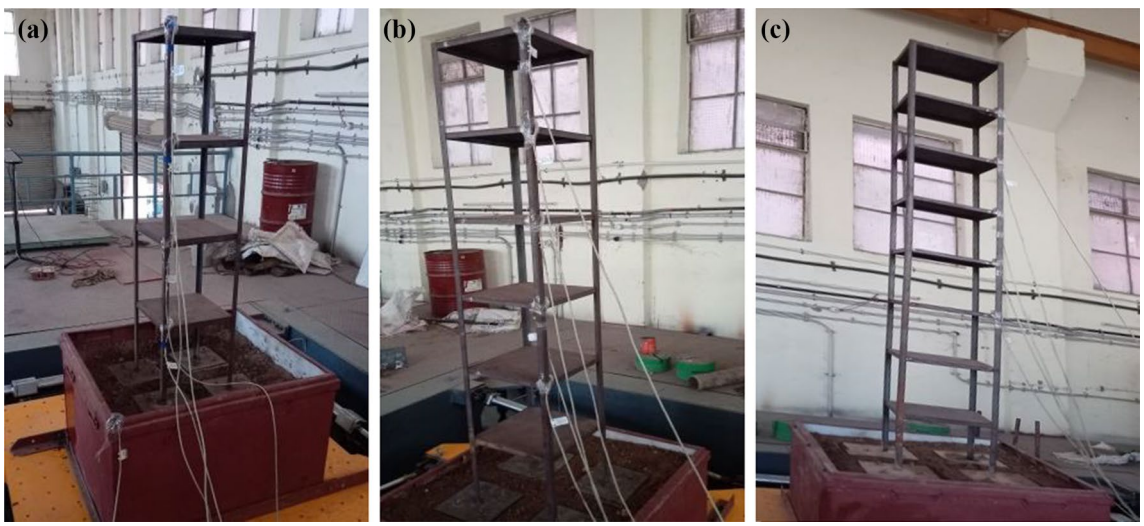


**Fig. 3** Experimental setup of frame models: (**a**) four-, (**b**) six-, and (**c**) eight-storey frame models on soil container and shake table

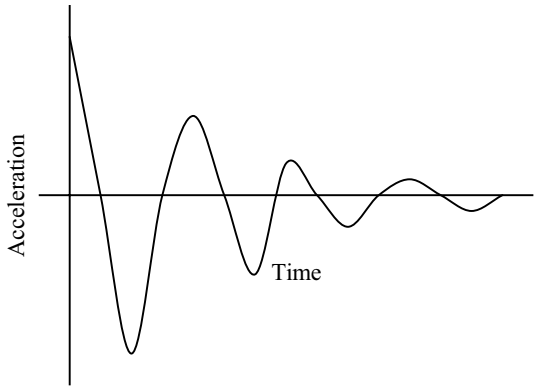


**Fig. 4** Typical free vibration acceleration record of the test model with fixed base

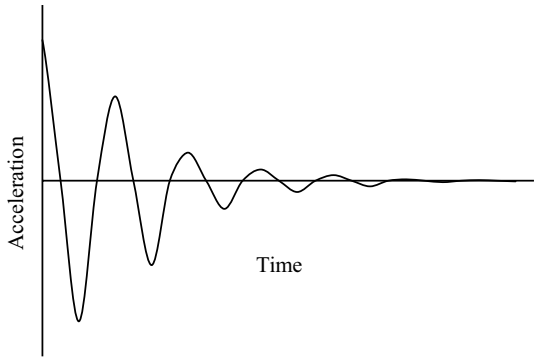


**Fig. 5** Typical free vibration acceleration record of the test model with isolated footing

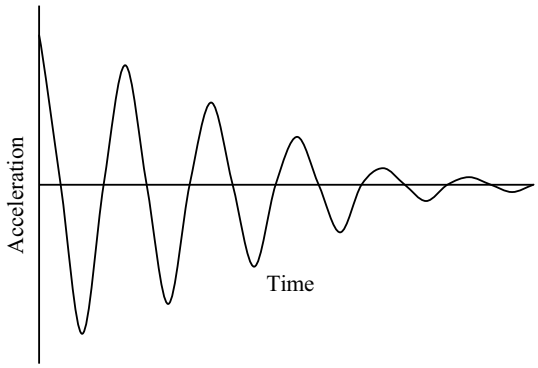


**Fig. 6** Typical free vibration acceleration record of the test model with mat footing

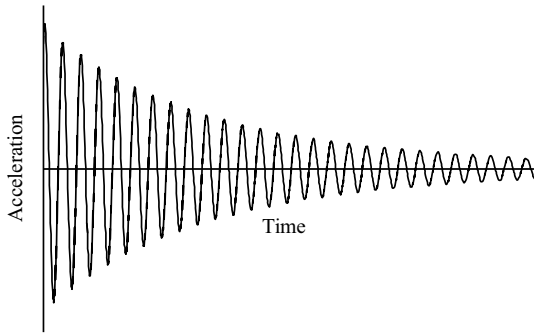


**Fig. 7** Typical free vibration acceleration record of the test model with pile foundation

## Damping from free vibration test

Because it is not possible to determine analytically the damping ratio ζ for practical structures, this property is determined experimentally. A common method of obtaining a damping coefficient is the log-decrement method from free vibration decay data in which the decrease in successive amplitudes of oscillation with increase in time gives information of damping present in the system. The decrease in amplitude over a certain number of cycles gives a good estimate of damping. The amplitudes considered may be of acceleration or of displacements plots. In this study, acceleration response has been used to measure the damping of the model using logarithmic decrement formula given by Eq. 2 (Sáez et al. 2013). In the free vibration test, an initial horizontal displacement was applied by pulling using a non-extensible rope to the structural model fixed on the shake table. The rope was suddenly cut and the resulting free vibration accelerations of the model were recorded by already fixed accelerometers at the floor levels.

$$\zeta = \frac{1}{2\pi j} \ln \frac{\ddot{u}_i}{\ddot{u}_{i+j}}, \tag{2}$$

where $j$ = number of cycles, $\ddot{u}_i$ = acceleration at $i$th peak, and $\ddot{u}_{i+j}$ = acceleration at $(i+j)$th peak.

In the first case, free vibration analysis was conducted for each frame model by fixing it with the shake table. In the second case, the frame models with different types of foundations were embedded in soil and the free vibration records were obtained. The typical free vibration acceleration records obtained from the experiment are shown in Figs. 4, 5, 6, and 7 for fixed base, isolated, mat, and pile foundation systems. The values of natural frequency and damping ratio obtained from these records for each case are presented in Tables 2, 3, and 4 for four-, six-, and eight-storey frame models.

**Table 2** Natural frequency and damping ratio of four-storey frame model

| Types of foundations | Fixed | Isolated | Mat | Pile#1 | Pile#2 |
|---|---|---|---|---|---|
| Natural frequency (rad/s) | 14.00 | 13.00 | 12.54 | 10.75 | 9.87 |
| Damping ratio (%) | 5.00 | 4.58 | 4.24 | 4.12 | 3.98 |

**Table 3** Natural frequency and damping ratio of six-storey frame model

| Types of foundations | Fixed | Isolated | Mat | Pile#1 | Pile#2 |
|---|---|---|---|---|---|
| Natural frequency (rad/s) | 12.00 | 11.04 | 10.64 | 9.10 | 8.52 |
| Damping ratio (%) | 3.95 | 3.10 | 3.58 | 2.84 | 2.46 |

**Table 4** Natural frequency and damping ratio of eight-storey frame model

| Types of foundations | Fixed | Isolated | Mat | Pile#1 | Pile#2 |
|---|---|---|---|---|---|
| Natural frequency (rad/s) | 9.00 | 8.28 | 7.90 | 6.89 | 6.21 |
| Damping ratio (%) | 2.67 | 2.40 | 2.51 | 2.29 | 2.05 |

From the free vibration acceleration records natural frequencies and damping ratios of the frame models were determined by counting the number of cycles and using Eq. 2. These values are presented in Tables 2, 3, and 4. It is seen that the natural frequencies of the frame models decrease with the increase in their height irrespective of the foundation types. Therefore, it can be inferred that increase in height of the structure makes it more flexible. Natural frequencies are also seen to be decreasing in the order of fixed–isolated–mat–pile foundation systems. Therefore, it can be further inferred that the structure turns flexible in the order of foundation types stated above. It is also seen that increasing depth of the pile adds to the flexibility of the structural system.

Regarding damping it is seen that the damping of the frame model also decreases with the increase in height. Further, with respect to the type of the foundation it is seen that for higher buildings (six and eight storeys) damping is more for mat foundation as compared to the isolated foundation. However, the damping is found to be less in case of piled foundation as compared to mat and isolated footings. It is further observed that the values of damping for all building heights decrease with the increase in pile depth.

An attempt was made to derive empirical relationships based on experimental data obtained for the estimation of damping ratio $\zeta$ in terms of building height when frame models are situated on different types of foundation systems (viz. isolated footing, mat footing, and pile foundations). Expression for $\zeta$ based on the best fit curve for the data was obtained. Several forms of expressions were tried for the best fit expression. However, the exponential form of the expression was obtained as a best fit curve of the experimental data. The obtained expressions for damping ratios are shown in Eqs. 3, 4, 5, and 6 with $R^2$ values 0.9996, 0.9152, 0.9954, and 0.9834, respectively, for isolated, mat, Pile#1, and Pile#2 foundation types.

For isolated footing:

$$\zeta = 47.77\, h^{-0.94}. \tag{3}$$

For mat footing:

$$\zeta = 23.3\, h^{-0.67}. \tag{4}$$

For pile#1 foundation:

$$\zeta = 35.31\, h^{-0.86}. \tag{5}$$

For pile#2 foundation:

$$\zeta = 50.51 h^{-1.03}. \tag{6}$$

Equations 3, 4, 5, 6 are valid for square symmetrical scaled steel frame model and selected soil conditions. For other type of building and soil conditions these equations may differ.

## Input motion

In this study, the acceleration time history and response values of the N–S component of El-Centro (California 1940) earthquake were used since the time history of N–S component of motion is available in digital form and is well studied and used by several researchers. The N–S component was preferred to the E–W component as the N–S component is more intense as compared to the E–W component. A more irregular response in the structure is expected to be generated because the N–S component of acceleration time history shows high irregularity in terms of acceleration. The highly irregular earthquake has been considered to investigate the effect of SSI on the response of the structural model. The N–S component of acceleration time history of the El-Centro earthquake is shown in Fig. 8. The frequency of El-Centro N–S input earthquake is 2.92 Hz. The absolute maximum amplitude of El-Centro N–S earthquake is

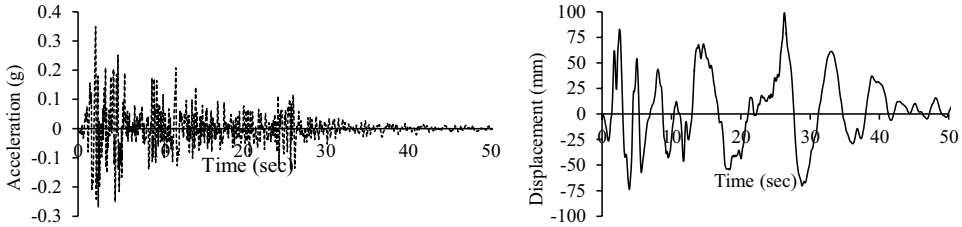


**Fig. 8** El-Centro N–S earthquake motion

0.319 g. The N–S component of El-Centro earthquake was applied to the shake table platform through its control panel which is capable of applying many types of standard as well as customized motions. The input motion in this case was applied at a time step of 0.01 s and for a total duration of 50 s.

## Results and discussion

This section summarizes main outcomes acquired from the experimental study of the frame models with and without the SSI effects. As observed from Tables 2, 3, and 4 for a given height of the building frame, fixed base building frame yields maximum frequency. However, fixed base buildings are seldom built. The piled foundation offers least frequency as compared to all other foundations in the presence of the SSI effect. For a given foundation type, the natural frequency of the frame model decreases with the increase in its height. As far as the damping is concerned, the taller building frame standing on a given type of footing has a lowest damping ratio. However, the pile foundation gives least damping ratio as compared to all other foundation systems irrespective of the height of the buildings. All output responses have been presented here for 50 s due to space limitation and also due to insignificant response characteristics after 50 s. The output responses of frame models to El-Centro earthquake input motion for fixed base, isolated footing, mat footing, and pile foundations were obtained in the N–S direction. Figures 9, 10, and 11 show the acceleration vs. time and displacement vs. time curves when structural models were of fixed base condition. For isolated footing, mat footing, and pile foundations (Pile#1 and Pile#2), the response plots in terms of displacement vs. time are presented in Figs. 12, 13, 14, and 15.

The values in Table 5 have also been plotted in Fig. 16 for more clarity. It is seen from Fig. 16 that all the building models with mat footing reach their maximum displacements earlier as compared to the models on the other footings. Also, the maximum acceleration response is found to take place when the frame model is situated on the isolated

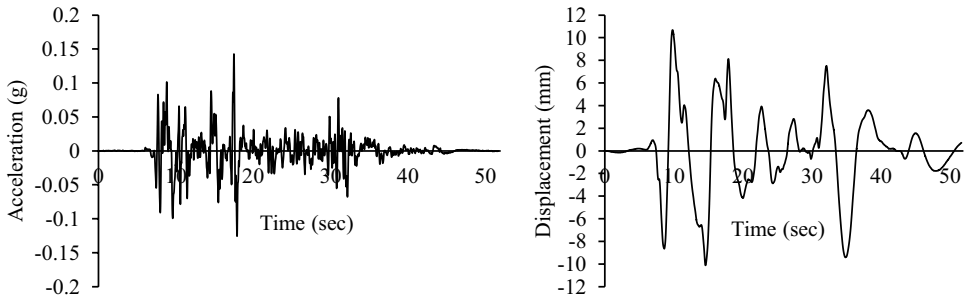


**Fig. 9** Top floor responses of eight-storey frame model due to El-Centro for fixed base condition

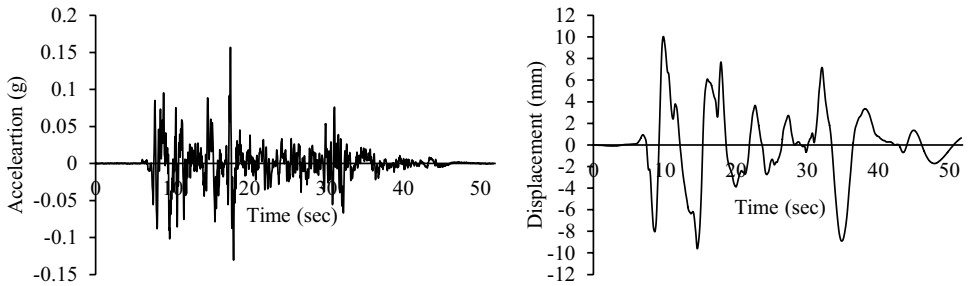


**Fig. 10** Top floor responses of six-storey frame model due to El-Centro for fixed base condition

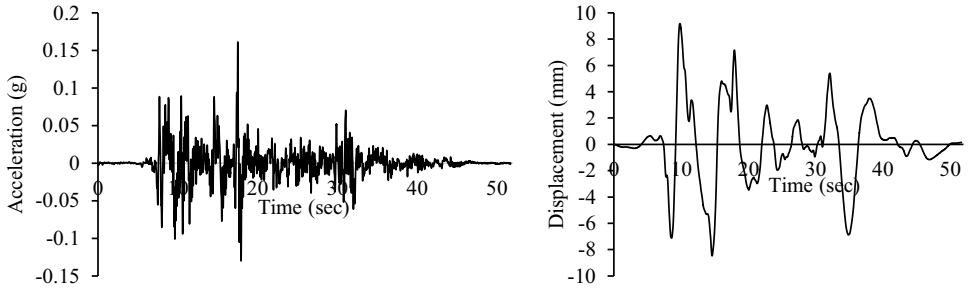


**Fig. 11** Top floor responses of four-storey frame model due to El-Centro for fixed base condition

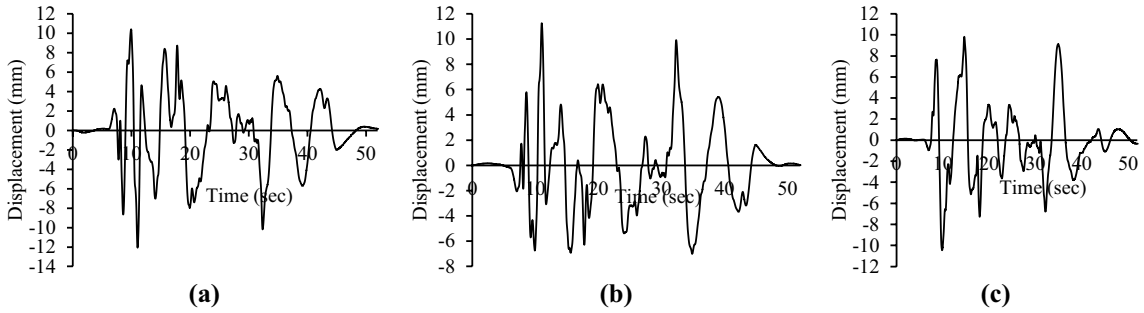


**Fig. 12** Top floor displacement responses of (**a**) eight-, (**b**) six-, and (**c**) four-storey frames due to El-Centro for isolated footing

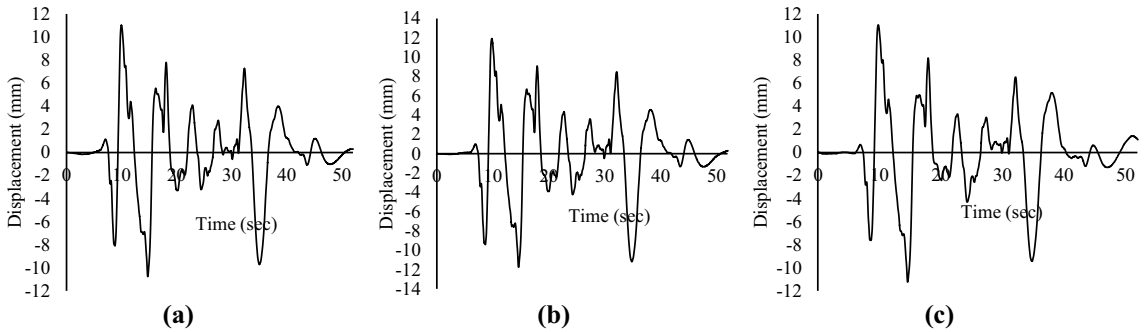


**Fig. 13** Top floor displacement responses of (**a**) eight, (**b**) six and (**c**) four storey due to El-Centro for mat footing

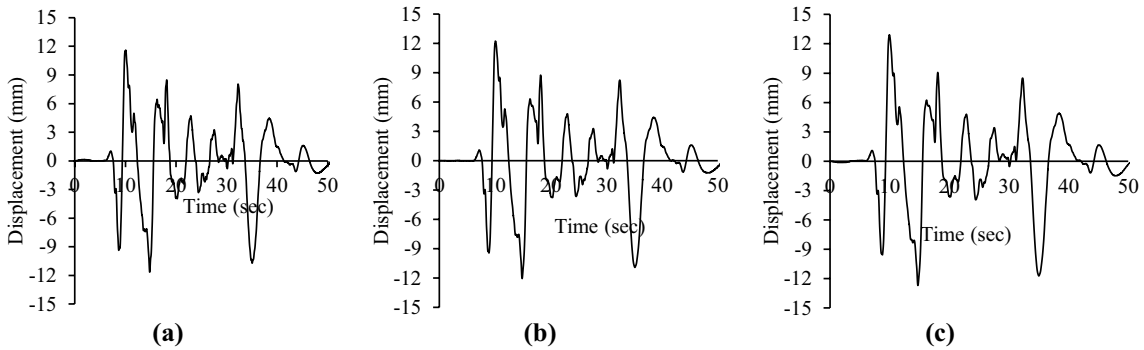


**Fig. 14** Top floor displacement responses of (**a**) eight, (**b**) six and (**c**) four storey due to El-Centro for pile#1 foundation

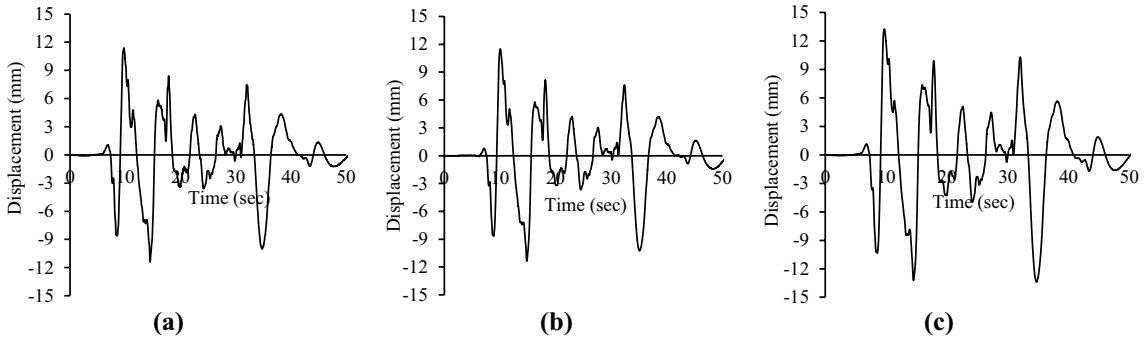


**Fig. 15** Top floor displacement responses of (**a**) eight, (**b**) six and (**c**) four storey due to El-Centro for pile#2 foundation

**Table 5** Peak displacement and maximum acceleration and their occurrence time experienced by frame models resting on different foundations

| Types of frame models | Foundation type | Maximum displacement (mm) | Occurrence time for maximum displacement (s) | Maximum acceleration (g) | Occurrence time for maximum acceleration (s) |
|---|---|---|---|---|---|
| Four storey | Fixed base | 9.18 | 9.51 | 0.1612 | 16.74 |
| | Isolated | 12.58 | 9.62 | 0.2248 | 16.89 |
| | Mat | 12.11 | 9.47 | 0.2207 | 16.88 |
| | Pile#1 | 11.79 | 9.78 | 0.2181 | 17.66 |
| | Pile#2 | 11.26 | 9.65 | 0.2045 | 17.32 |
| Six storey | Fixed base | 10.04 | 9.39 | 0.1568 | 16.81 |
| | Isolated | 12.89 | 10.46 | 0.2787 | 7.84 |
| | Mat | 12.41 | 9.51 | 0.2616 | 16.91 |
| | Pile#1 | 11.95 | 10.10 | 0.2401 | 17.67 |
| | Pile#2 | 11.48 | 10.31 | 0.2460 | 17.66 |
| Eight storey | Fixed base | 10.68 | 9.65 | 0.1425 | 16.95 |
| | Isolated | 13.15 | 10.76 | 0.2875 | 8.17 |
| | Mat | 12.78 | 9.62 | 0.2651 | 17.06 |
| | Pile#1 | 12.01 | 10.10 | 0.2408 | 17.92 |
| | Pile#2 | 11.67 | 9.76 | 0.2345 | 17.48 |

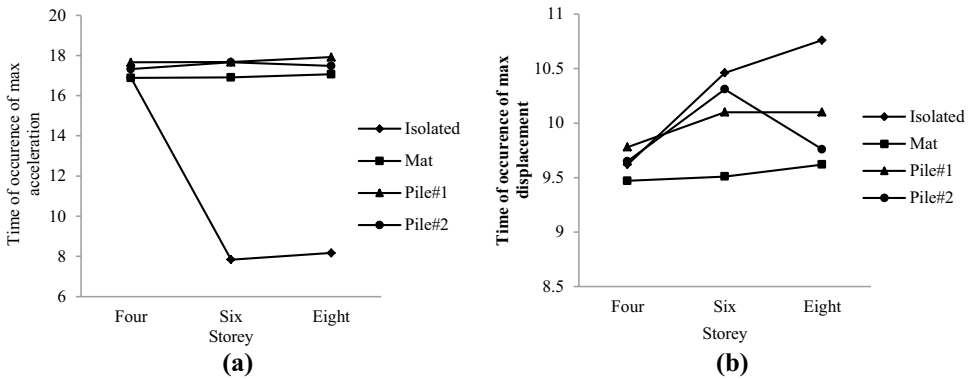


**Fig. 16** Peak displacement and maximum acceleration and their occurrence time experienced by frame models resting on different foundations

footing system. It is also found that the maximum displacement takes place in case of isolated footing system for all frame heights. It is seen that for a particular height of frame model the isolated footing gives the maximum displacement, whereas the Pile#2 (the deeper pile) gives the least displacement at a later time. The peak displacements and accelerations, and their occurrence times experienced by the frame models are presented in Table 5. Comparison of maximum displacements for different foundations is shown in Fig. 17. Clearly, the maximum displacements for all building heights tend to decrease in the order of isolated–mat–pile foundation systems and this decrease is almost at a uniform rate. It is found that fixed base offers less displacement as compared to all other types of foundation systems. Also deeper pile (Pile#2) yields lesser displacement at the top floor as compared to other type of foundation systems, e.g., isolated, mat, and Pile#1. A similar trend of decreasing displacement was also presented by Tang et al. (2014) and Luo et al. (2016) in

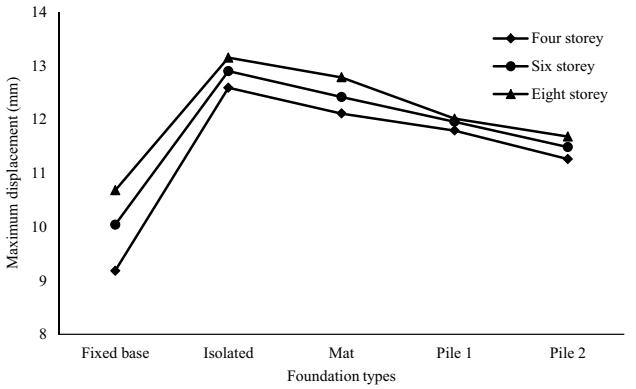


**Fig. 17** Comparative maximum displacement and types of foundation system

their studies. These investigations broadly corroborate our experimental results also.

## Summary and conclusion

In this paper, results of the experimental study on three scaled steel frame models of four-, six-, and eight-storeyed buildings have been presented. The comparative study of natural frequencies, damping ratios, acceleration, and displacement responses for different foundations such as isolated, mat, and pile foundations have been carried out considering SSI effect. Also, two different pile depths have been taken to study the effect of pile depths on response characteristics. It is seen that both the natural frequency and damping ratio are maximum in case of the fixed base condition. However, since fixed base buildings are rarely possible more emphasis is given towards isolated, mat, and pile foundations. Pile foundation offers longest time period as compared to all other foundations in the presence of SSI effect. For a given foundation type, the time period of a frame model increases with the increase in height of frame model. Concerning damping, the taller building frame standing on a given type of footing is found to have lower damping ratio. However, the pile foundation gives least damping ratio as compared to all other foundation systems irrespective of the heights of buildings. It is clearly shown that both the natural frequency and the damping ratio depend on the foundation systems of the frame models. It has been found that fixed base offers least lateral displacement as compared to all other types of foundations. However, pile foundation offers least lateral displacement of the frame models amongst isolated, mat, and pile foundations. The displacement responses of building frame models are increasing with increase in height.

### Compliance with ethical standards

**Conflict of interest** On behalf of all the authors the corresponding author states that there is no conflict of interest.

## References


Badry, P., & Satyam, N. (2016). Seismic soil structure interaction analysis for asymmetrical buildings supported on piled raft for the 2015 nepal earthquake. *Journal of Asian Earth Sciences*. https://doi.org/10.1016/j.jseaes.2016.03.014.

California (1940). El Centro NS component. http://www.vibrationdata.com/elcentro_NS.dat.

Chau, K. T., Shen, C. Y., & Guo, X. (2009). Nonlinear seismic soil-pile-structure interactions: shaking table tests and fem analyses. *Soil Dynamics and Earthquake Engineering, 29,* 300–310. https://doi.org/10.1016/j.soildyn.2008.02.004.

Chen, M. C., Astroza, R., Restrepo, J. I., et al. (2017). Predominant period and equivalent viscous damping ratio identification for a full-scale building shake table test. *Earthquake Engineering and Structural Dynamics, 46,* 2459–2477. https://doi.org/10.1002/eqe.2913.

Chopra, A. K. (1995). *Dynamics of structure*. New Jersey: Prentice Hall Inc., Englewood Cliffs. ISBN 0-13-855214-2.

Chu, D, Truman, K. Z. (2004) Effects of pile foundation configurations in seismic soil-pile-structure interaction. In: 13th World Conf Earthq Eng Paper No. 1551.

Durante, M. G., Di Sarno, L., Sica, S., et al (2013) Seismic pile-soil interaction: Experimental results vs. numerical simulations. ECCOMAS Themat Conf—COMPDYN 2013 4th Int Conf Comput Methods Struct Dyn Earthq Eng Proc—An IACM Spec Interes Conf 1218–1229.

Gallipoli, M. R., Mucciarelli, M., & Vona, M. (2009). Empirical estimate of fundamental frequencies and damping for Italian buildings. *Earthquake Engineering and Structural Dynamics, 38,* 973–988. https://doi.org/10.1002/eqe.

Ge, Q., Xiong, F., Zhang, J., & Chen, J. (2016). Shaking table test of dynamic interaction of soil—high-rise buildings. *European Journal of Environmental and Civil Engineering, 21,* 249–271. https://doi.org/10.1080/19648189.2015.1110057.

Hokmabadi, A. S., Fatahi, B., & Samali, B. (2015). Physical modeling of seismic soil-pile-structure interaction for buildings on soft soils. *International Journal of Geomechanics, 15,* 04014046. https://doi.org/10.1061/(ASCE)GM.1943-5622.0000396.

Hosseinzadeh, N., Davoodi, M., Rayat Roknabadi, E. (2012) Shake Table Study of Soil Structure Interaction Effects in Surface and Embedded Foundations. In: 15th World Conference on Earthquake Engineering (15WCEE).

Indian Standard. IS 808 : 1989 Dimensions for hot rolled steel beam, column, channel and angle sections. 1989.

Indian Standard. IS : 1498—1970, Classification and identification of soils for general engineering purposes, bureau of indian standards, New Delhi (ReaffIrmed 2007). 2000.

Kampitsis, A. E., Giannakos, S., Gerolymos, N., & Sapountzakis, E. J. (2015). Soil-pile interaction considering structural yielding: Numerical modeling and experimental validation. *Engineering Structures, 99,* 319–333. https://doi.org/10.1016/j.engstruct.2015.05.004.

Lu, X., Chen, Y., Chen, B., & Li, P. (2002). Shaking table model test on the dynamic soil-structure interaction system. *Journal of Asian Architecture and Building Engineering, 1,* 55–64.

Luo, C., Yang, X., Zhan, C., et al. (2016). Nonlinear 3D finite element analysis of soil-pile-structure interaction system subjected to horizontal earthquake excitation. *Soil Dynamics and Earthquake Engineering*. https://doi.org/10.1016/j.soildyn.2016.02.005.

Mishra, S. S. (2017). Time period estimation of rc frame buildings through soil stiffness modeling. *Journal of The Institution of Engineers, 98,* 303–310. https://doi.org/10.1007/s40030-017-0224-0.

Sáez, E., Lopez-Caballero, F., & Modaressi-Farahmand-Razavi, A. (2013). Inelastic dynamic soil-structure interaction effects on moment-resisting frame buildings. *Engineering Structures, 51,* 166–177. https://doi.org/10.1016/j.engstruct.2013.01.020.

Saha, R., Dutta, S. C., & Haldar, S. (2015). Seismic response of soil-pile raft-structure system. *Journal of Civil Engineering and Management, 21,* 144–164. https://doi.org/10.3846/13923730.2013.802716.

SeismoSignal v.4.3.0. Seismosoft Ltd. (2011). http://www.seismosoft.com. Accessed July 2018.

Tabatabaiefar, S. H. R., Fatahi, B., & Samali, B. (2014). Numerical and experimental investigations on seismic response of building frames under influence of soil-structure interaction. *Advances in Structural Engineering, 17,* 109–130. https://doi.org/10.1260/1369-4332.17.1.109.

Tabatabaiefar, H. R., & Massumi, A. (2010). A simplified method to determine seismic responses of reinforced concrete moment resisting building frames under influence of soil-structure interaction. *Soil Dynamics and Earthquake Engineering, 30,* 1259–1267. https://doi.org/10.1016/j.soildyn.2010.05.008.

Tang, L., Maula, B. H., Ling, X., & Su, L. (2014). Numerical simulations of shake-table experiment for dynamic soil-pile-structure interaction in liquefiable soils. *Earthquake Engineering and Engineering Vibration, 13,* 171–180. https://doi.org/10.1007/s11803-014-0221-5.

Turan, A., Hinchberger, S. D., & El Naggar, H. (2009). Design and commissioning of a laminar soil container for use on small shaking tables. *Soil Dynamics and Earthquake Engineering, 29,* 404–414. https://doi.org/10.1016/j.soildyn.2008.04.003.

Wolf, J. P. (1985). *Dynamic soil-structure interaction* (p. 07632). New Jersey: Prentice-Hall Inc.